Experimental investigation of co-flow jet's airfoil flow control by hot wire anemometer

View Online   Export Citation   CrossMark

A. Bahrami,[1] S. Hoseinzadeh,[2,3,a] (iD) P. S. Heyns,[2] (iD) and S. M. Mirhosseini[4]

AFFILIATIONS

[1] School of Mechanical Engineering, Iran University of Science and Technology, Tehran, Iran
[2] Centre for Asset Integrity Management, Department of Mechanical and Aeronautical Engineering, University of Pretoria, Pretoria 0081, South Africa
[3] Young Researchers and Elite Club, West Tehran Branch, Islamic Azad University, Tehran, Iran
[4] Department of Mechanical Engineering, Hakim Sabzevari University, Sabzevar, Khorasan 9617976487, Iran

[a] Author to whom correspondence should be addressed: Hoseinzadeh.siamak@gmail.com

ABSTRACT

An experimental flow control technique is given in this paper to study the jet effect on the coflow jet's airfoil with injection and suction and compared with the jet-off condition. The airfoil is CFJ0025-065-196, and the Reynolds number based on the airfoil's chord length is 10^5. To measure the turbulence components of flow, a hot wire anemometry apparatus in a wind tunnel has been used. In this paper, the effect of the average velocity and boundary layer thickness on the coflow jet's airfoil is analyzed. The test is done for two different coflow velocities and for different angles of attack. It is also shown that, by increasing the velocity difference between the jet and the main flow, separation is delayed, and this delay can be preserved by raising coflow velocity at higher angles of attack. So, this flow control method has a good efficiency, and it is possible to reach higher numbers of lift and lower numbers of drag coefficients.

Published under license by AIP Publishing. https://doi.org/10.1063/1.5113592

NOMENCLATURE

x, y chord and normal directions, with respect to the airfoil (mm)
c chord length (mm)
AOA angle of attack
CFJ coflow jet
u mean velocity in the chord direction (m/s)
δ_w boundary layer thickness (mm)

I. INTRODUCTION

Flow control plays an important role in engineering and industrial applications, such as enhancing the efficiency of aircraft aerodynamics and addressing the energy consumption issues.[1–10] By reviewing studies that have been done on the new flow control in the past few decades,[11–19] the necessity of studying this phenomenon by considering the turbulent flow has been felt strongly because the turbulent flow has high importance in the momentum mixing.[20] In most cases, in order to control the flow on the airfoils, the wall jet is used for more mixing of fluid momentum between the jet and the main flow. Zha et al.[14,21–25] developed a new flow control on this basis that results in an increase in the lift coefficient and stall margin and a decrease in the drag coefficient on the airfoil and delay time of stall by raising the diffusion factors in compressor blades.

The coflow jet's airfoil has an injection slot near the leading edge and a suction slot near the trailing edge on the airfoil suction surface. The turbulent shear layer between the main flow and the jet one causes turbulence diffusion and strong mixing under adverse pressure gradient, which enhances latent transport of energy from the jet to the main flow and allows the main flow to overcome adverse pressure gradient and remain attached at a high angle of attack (AOA).[26] Also, by increasing the velocity of jet flow, the created delay in the flow separation is raised.

In this paper, the flow rate of injection is higher than that of suction because the effect of injection on the performance of this type of flow controlling is more than that of suction.[16,27] In addition, instead of velocity, the pressure has been kept constant
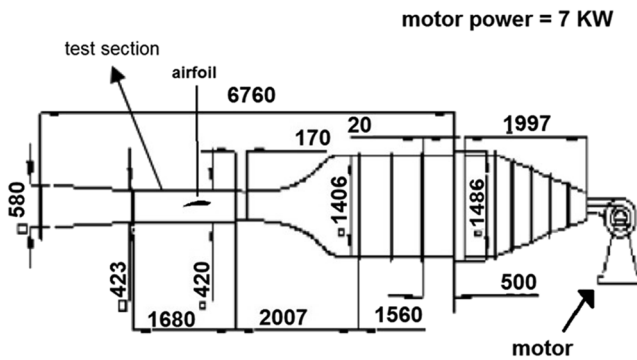
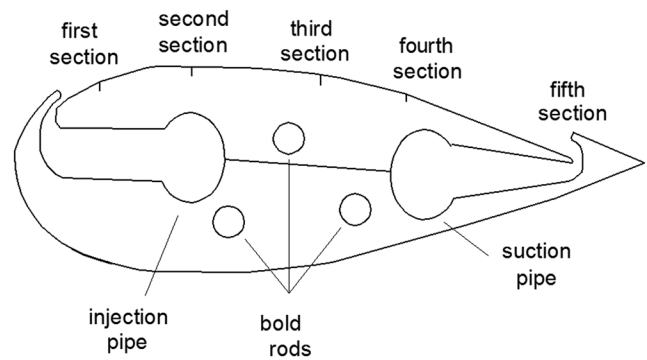FIG. 1. Schematic of the wind tunnel (dimensions are in millimeters).

FIG. 2. Section of the CFJ0025-065-196 airfoil.

in the injection slot and at various angles of attack. In the simplest case, the high pressure flow blown from the compressor outlet is injected on the airfoil by a constant working pressure without the use of any control valve to maintain the mass flow rate constant.

II. EXPERIMENTAL SETUP AND MEASUREMENT TECHNIQUES

All airflow and aerodynamic variables were acquired from Hakim Sabzevari University's 7 kW wind tunnel equipped with a one-dimensional hot wire anemometry apparatus. Figure 1 shows an

overview of this wind tunnel dimension and the CFJ airfoil, while the turbulent intensity of this device is less than 1%. A compressor supplies the injection flow, and the injection and suction flow conditions were independently controlled.

The airfoil used in this test is CFJ0025-065-196 airfoil, as mentioned in the literature.[23,28] To ensure a uniform injection and suction in the whole slot, a new internal design has been used. A schematic of a CFJ airfoil concept is shown in Fig. 2. In this airfoil, there is a porous pipe with many holes in airfoil's length. So that in injection pipe inside the airfoil, the sum of open surfaces of holes increases as it takes distance from air entrance and opposite takes place for the suction tube.
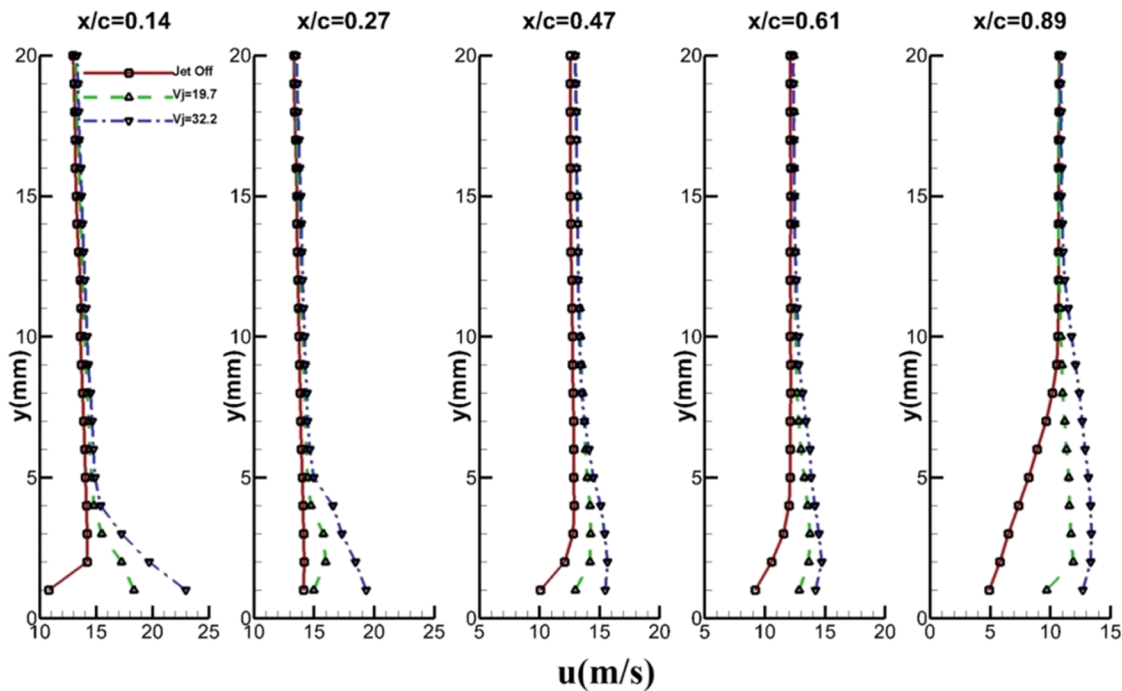

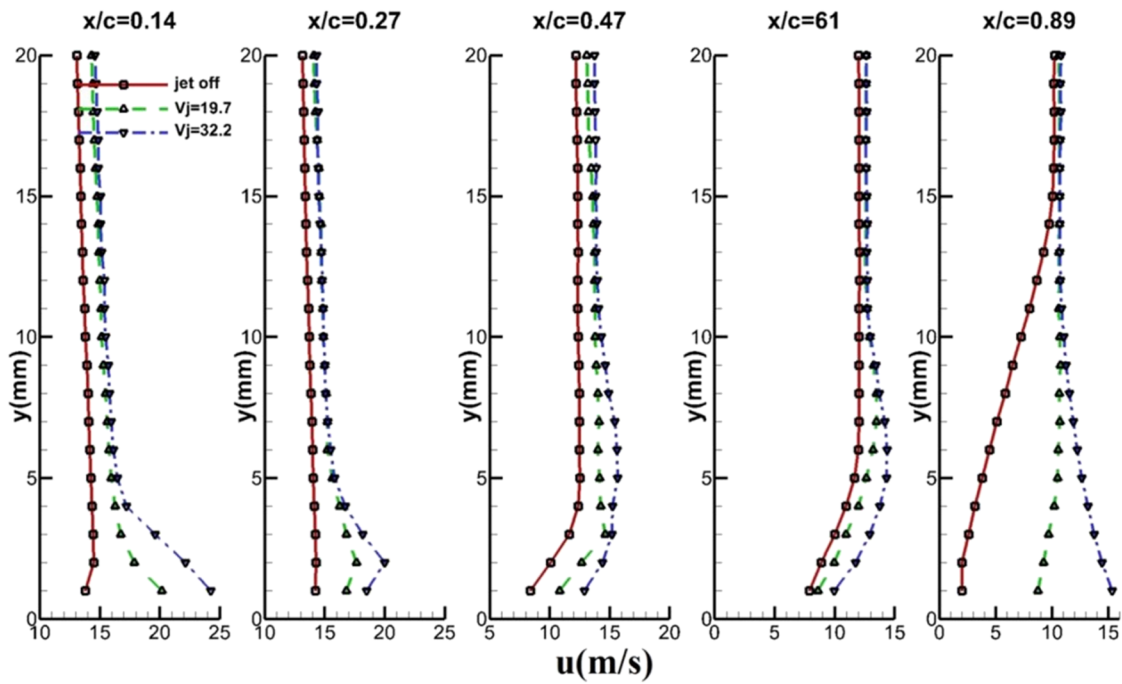FIG. 3. Average velocity profile for AOA = 0°.

FIG. 4. Average velocity profile for AOA = 5°.

A 250 l/min compressor has been used to generate injection and suction, which is single-phased and has two cylinders. The injection for this compressor is provided from the airfoil suction slot, and the mass flow rate of this suction is constant. But the injection air is blown in two different modes; for the first mode, the partial pressure is 598 Pa and the jet velocity is 19.7 m/s, while for the second mode, the partial pressure is 1596 Pa and the jet velocity is 32.2 m/s. Also, the partial pressure for suction is 1596 Pa. The data are
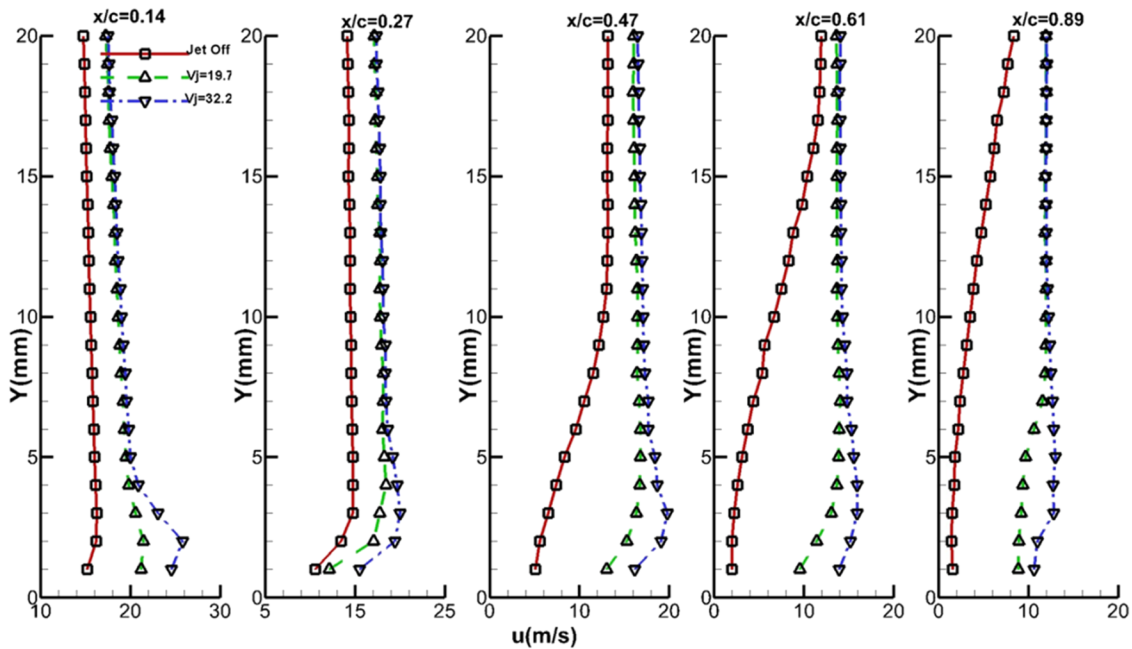

FIG. 5. Average velocity profile for AOA = 12°.

TABLE I. Thickness of the boundary layer for different values of attack angle.

Attack angle	Mode	δ_W in situations (mm)			
		2	3	4	5
	Off mode		2	2	5
	On mode 1				2
5	Off mode		3	4	13
	On mode 1		2	5	3
	On mode 2			3	
12	Off mode		7	15	22
	On mode 1		2	2	5
	On mode 2				2
20	Off mode	23			
	On mode 1	2	3	5	17
	On mode 2			2	5
25	On mode 1	2	5	20	48
	On mode 2	3	3	10	24
30	On mode 1	5	14	25	43
	On mode 2	4	3	25	38

acquired in five stations that are placed at x/c = 0.14, x/c = 0.27, x/c = 0.47, x/c = 0.61, and x/c = 0.89, where the cord length is 15 cm and x is the distance from the injection slot in line with the chord.
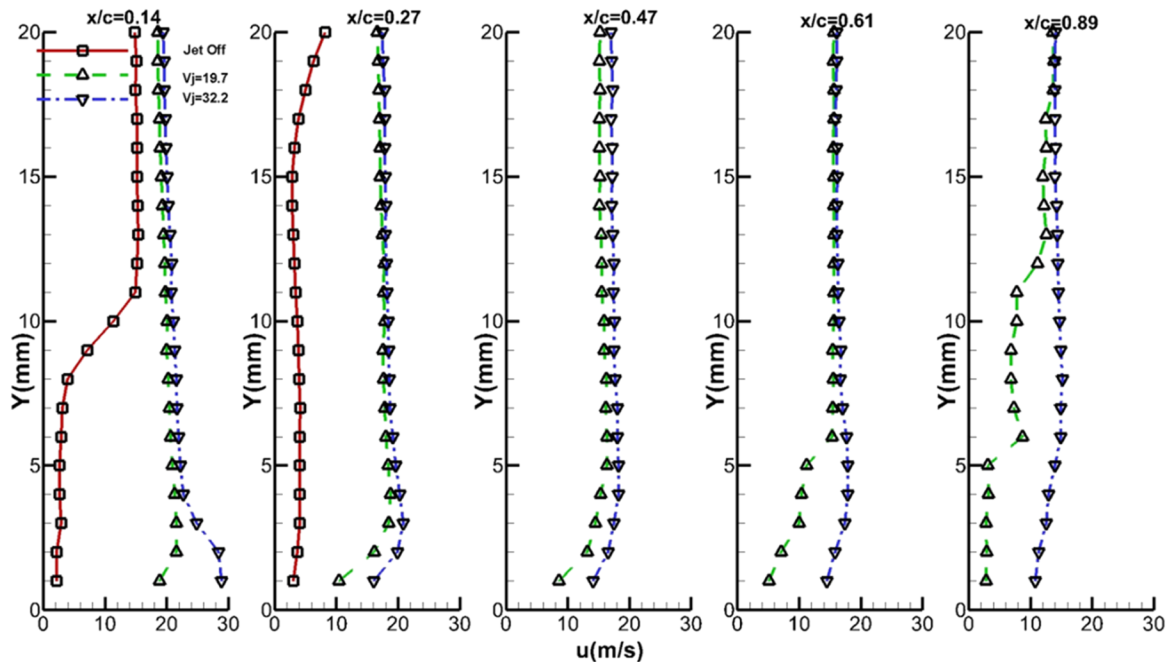
III. RESULTS AND DISCUSSION

A. Average velocity profiles

Figure 3 shows the diagram of average velocity on the CFJ airfoil in terms of vertical distance. The horizontal axis is for mean velocity profiles (meters per second), and the vertical axis is for the distance from the airfoil surface (millimeters). Also, each station is shown on the top of graphs.

In the entire picture, the bold line is for the jet-off mode, the dashed line is for the jet 1 "on" mode, and the dotted one indicates jet 2 "on" mode. By examining Fig. 3, it can be seen that the maximum velocity of the jet decreases, while the jet wall layer increases; in other words, the jet gets wider and gives its momentum to the main flow.[20]

In the first stations, due to lower thickness of the boundary layer, only the top layer of the jet is shown in Fig. 3. Barenblatt introduced three layers for the jet wall: the wall layer, the mixing layer, and the top layer where layers 1 and 3 are separated by layer 2.[29]

Figures 4 and 5 demonstrate that, by increasing attack angle, a considerable difference between the jet off mode velocity and the jet on mode velocity takes place. This difference reveals the displacement of the stagnation point toward the trailing edge on the airfoil pressure surface as well as an increase in circulation.

Table I gives the thickness of the boundary layer for the jet off mode and two jet on modes. As it could be seen in Table I, by taking distance from injection slot towards trailing edge, the more thickness of boundary layer and jet appears.

Looking at the thickness of the boundary layer for the jet off mode and attack angle of 5, it can be found that δ_W = 4 mm in station 4 becomes δ_W = 13 mm in station 5, and this sudden growth

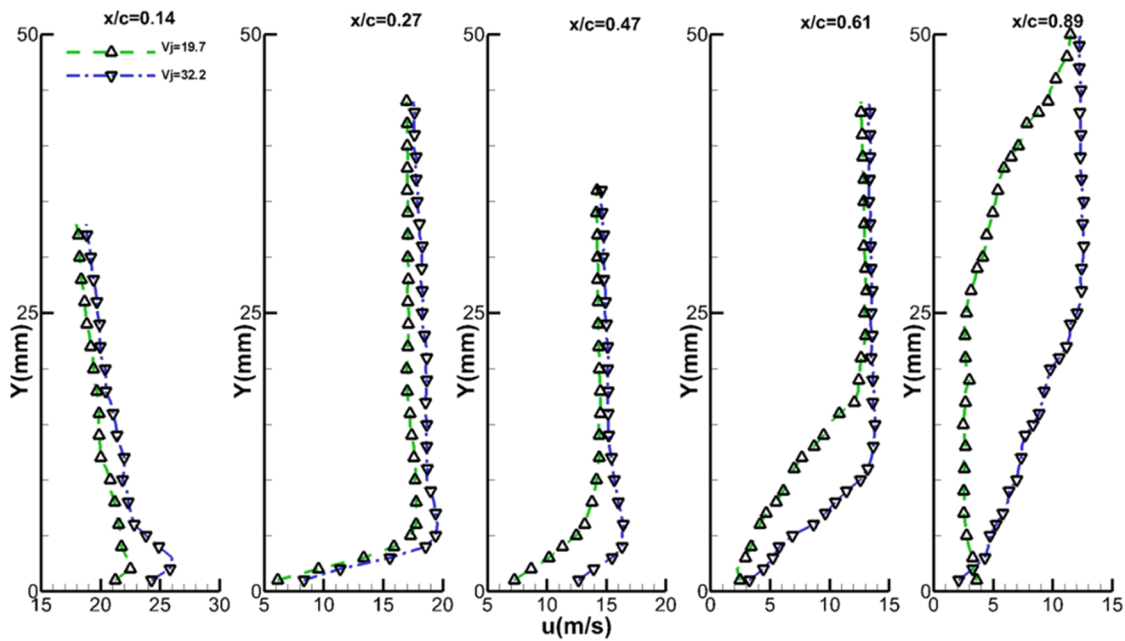FIG. 6. Average velocity profile for AOA = 20°.

FIG. 7. Average velocity profile for AOA = 25°.

could be due to separation of flow. This point could be seen in Fig. 4 showing the average velocity profile by raising the angle of attack. Table I shows this sudden growth in boundary layer thickness by jet off mode too, while the flow is attached for the two jet on modes, but

this growth is occurred one station sooner that is between 3 and 4. In fact by increasing the angle of attack, the flow is unable to dominate the adverse pressure gradient, while the CFJ flow control method helps the flow remain attached by giving energy to the flow. So, the
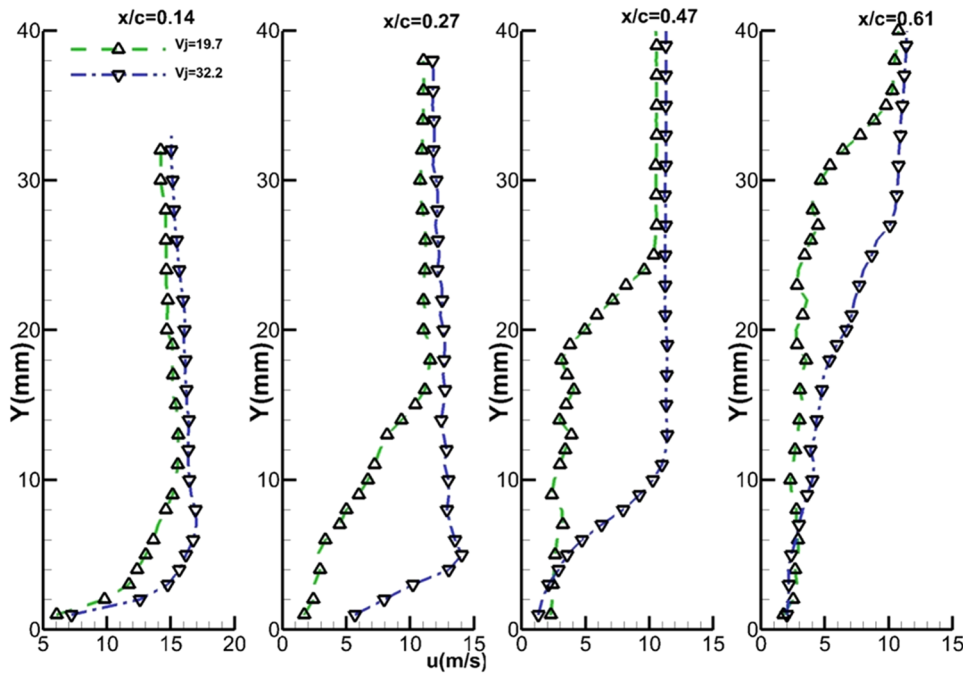

FIG. 8. Average velocity profile for AOA = 30°.

lift coefficient will be increased while the drag coefficient decreases. This could be seen in Fig. 5 where the velocity profile is shown at an attack angle of 12.

For an attack angle of 20, the thickness of the boundary layer in Fig. 6 and Table I indicates the high growth in both first and second stations because of flow separation. When the attack angle is changed to 25, it is observed that there is no difference between the velocity of the jet and main flow. Due to massive separation of flow and stall at an attack angle of 20° in the jet off mode, no further data are required. As seen in Table I, a sudden growth of the boundary layer between stations 3 and 4 occurs in both jet on modes. This growth in the first jet on mode is faster than that in the second mode, as it could be seen in Fig. 7, and it is because of the less energy in mode 1. At an attack angle of 30, the velocity difference between the jet and the main flow disappears earlier, and as seen in Fig. 8, the sudden growth of the boundary layer for mode 1 occurs between stations 1 and 2, while for mode 2, it is between stations 2 and 3. So, it is understandable that, for avoiding separation, the coflow jet's airfoil should have a very good operation; as for attack angles lower than 20, the first type with a partial pressure of 598 Pa and a jet velocity of 19.7 m/s is enough. But for an angle attack of 20° or more, the second type with a partial pressure of 1596 Pa and a jet velocity of 32.2 m/s is more proper.

Yarusevych *et al.* had studied the flow on the CFJ0025-065-196 airfoil with similar Reynolds number in two experimental papers, one of those by using a hot wire anemometer and the other by using the smoke wire technique.[30] They observed a slight flow separation at an attack angle of 5° that is very close to that in this study. In fact, the separation took place on airfoil CFJ0025-065-196 at a little closer point to the leading edge, which is caused by the difference in the geometry of the two airfoils.

IV. CONCLUSIONS

In this paper, the coflow jet's airfoil flow control method has been used to show the effect of an auxiliary flow inside an airfoil compared with the jet-off condition. The experiment has been done with a hot wire anemometry apparatus in a wind tunnel on airfoil CFJ0025-065-196 at the Reynolds number of 105 based on the airfoil's chord length. It is shown that the boundary layer's thickness has had a good importance because the flow through this airfoil and mixing process with the main flow change its value and the place of separation. Furthermore, this test reveals the importance of jet velocity by showing that the more the difference between jet velocity and main flow, the more the delay created in the flow separation. So, the new flow control of CFJ has good efficiency because this delay is responsible for increasing the lift and decreasing the drag coefficients. In addition, as seen in this test, up to the attack angle of 30°, no full stall has occurred.

REFERENCES

[1] M. Gad-el Hak, "Flow control: The future," J. Aircr. **38**(3), 402–418 (2001).

[2] M. Sheikholeslami and O. Mahian, "Enhancement of PCM solidification using inorganic nanoparticles and an external magnetic field with application in energy storage systems," J. Cleaner Prod. **215**, 963–977 (2019).

[3] S. Hoseinzadeh, A. Moafi, A. Shirkhani, and A. J. Chamkha, "Numerical validation heat transfer of rectangular cross-section porous fins," J. Thermophys. Heat Transfer **33**(3), 698–704 (2019).

[4] S. Hoseinzadeh, R. Ghasemiasl, D. Havaei, and A. J. Chamkha, "Numerical investigation of rectangular thermal energy storage units with multiple phase change materials," J. Mol. Liq. **271**, 655–660 (2018).

[5] S. Hoseinzadeh, P. S. Heyns, A. J. Chamkha, and A. Shirkhani, "Thermal analysis of porous fins enclosure with the comparison of analytical and numerical methods," J. Therm. Anal. Calorim. **138**, 727–735 (2019).

[6] S. Hoseinzadeh, S. A. R. Sahebi, R. Ghasemiasl, and A. R. Majidian, "Experimental analysis to improving thermosyphon (TPCT) thermal efficiency using nanoparticles/based fluids (water)," Eur. Phys. J. Plus **132**, 197 (2017).

[7] S. Hoseinzadeh, M. Hadi Zakeri, A. Shirkhani, and A. J. Chamkha, "Analysis of energy consumption improvements of a zero-energy building in a humid mountainous area," J. Renewable Sustainable Energy **11**, 015103 (2019).

[8] A. Yari, S. Hoseinzadeh, A. A. Golneshan, and R. Ghasemiasl, "Numerical simulation for thermal design of a gas water heater with turbulent combined convection," in *ASME International* (ASME, 2015), p. V001T03A007.

[9] M. Sheikholeslami, "New computational approach for exergy and entropy analysis of nanofluid under the impact of Lorentz force through a porous media," Comput. Methods Appl. Mech. Eng. **344**, 319–333 (2019).

[10] M. Sheikholeslami, "Numerical approach for MHD Al_2O_3-water nanofluid transportation inside a permeable medium using innovative computer method," Comput. Methods Appl. Mech. Eng. **344**, 306–318 (2019).

[11] M. Sheikholeslami, M. B. Gerdroodbary, R. Moradi, A. Shafee, and Z. Li, "Application of neural network for estimation of heat transfer treatment of Al_2O_3-H_2O nanofluid through a channel," Comput. Methods Appl. Mech. Eng. **344**, 1–12 (2019).

[12] T. Barbaryan, S. Hoseinzadeh, P. Heyns, and M. Barbaryan, "Developing a low-fluid pressure safety valve design through a numerical analysis approach," Int. J. Numer. Methods Heat Fluid Flow (2019).

[13] S. Hoseinzadeh, P. Heyns, and H. Kariman, "Numerical investigation of heat transfer of laminar and turbulent pulsating Al_2O_3/water nanofluid flow," Int. J. Numer. Methods Heat Fluid Flow (2019).

[14] G.-C. Zha and C. Paxton, "A novel airfoil circulation augment flow control method using co-flow jet," NASA CP-2005-213509, 2005; also AIAA Paper 2004-2208, 2004.

[15] G.-C. Zha, W. Gao, and C. D. Paxton, "Jet effects on co-flow jet airfoil performance," AIAA J. **45**(6), 1222–1231 (2007).

[16] B.-Y. Wang and G.-C. Zha, "Detached-eddy simulation of a co-flow jet airfoil at high angle of attack," AIAA Paper 2009-4015, 2009.

[17] B. Dano, A. Lefebvre, and G.-C. Zha, "Experimental investigation of jet mixing mechanism of co-flow jet airfoil," AIAA Paper 2010-4421, 2010.

[18] H.-S. Im, G.-C. Zha, and B. P. E. Dano, "Large eddy simulation of coflow jet airfoil at high angle of attack," J. Fluids Eng. **136**(2), 021101 (2014).

[19] H. Mitsudharmadi and Y. Cui, "Implementation of co-flow jet concept on low Reynolds number airfoil," AIAA Paper 2010-4717, 2010.

[20] S. B. Pope, *Turbulent Flows* (Cambridge University Press, Cambridge, England, 2000).

[21] C. Paxton, G.-C. Zha, and D. Car, "Design of the secondary flow system for a co-flow jet cascade," AIAA Paper 2004-3928, 2004.

[22] D. Car, N. J. Kuprowicz, J. Estevadeordal, G.-C. Zha, and W. Copenhaver, "Stator diffusion enhancement using a re-circulating co-flowing steady jet," in *ASME TURBO EXPO, 14–17 June 2004* (ASME, 2004), ASME Paper GT2004-53086.

[23] G.-C. Zha, B. Carroll, C. Paxton, A. Conley, and A. Wells, "High performance airfoil using co-flow jet flow control," AIAA Paper 2005-1260, 2005.

[24] Y. Shi, J. Bai, J. Hua, and T. Yang, "Numerical analysis and optimization of boundary layer suction on airfoils," Chin. J. Aeronaut. **28**(2), 357–367 (2015).

[25] J. Lei, G. Feng, and H. Can, "Numerical study of separation on the trailing edge of a symmetrical airfoil at a low Reynolds number," Chin. J. Aeronaut. **26**(4), 918–925 (2013).

[26] W. Gao, A. Palewicz, G.-C. Zha, and C. D. Paxton, "Numerical investigation of co-flow jet airfoil with injection only," AIAA Paper 2006-1061, 2006.

[27]B. Wang, B. Haddoukessouni, J. Levy, and G.-C. Zha, "Numerical investigation of injection slot size effect on the performance of co-flow jet airfoil," AIAA Paper 2007-4427, 2007.

[28]G.-C. Zha and W. Gao, "Analysis of jet effects on co-flow jet airfoil performance with integrated propulsion system," AIAA Paper 2006-102, 2006.

[29]G. I. Barenblatt, A. J. Chorin, and V. M. Prostokishin, "The turbulent wall jet: A triple-layered structure and incomplete similarity," Proc. Natl. Acad. Sci. U. S. A. **102**(25), 8850–8853 (2005).

[30]S. Yarusevych, P. E. Sullivan, and J. G. Kawall, "Investigation of airfoil boundary layer and wake development at low Reynolds numbers," AIAA Paper 2004-2551, 2004.